# Ultra-broadband IF/LO system of NTU W-band interferometer array

Hsiao-Feng Teng[a], Jing-Cheng Wu[a], Huan-Hsin Li[a], Tzi-Hong Chiueh[a], Dou-Chih Niu[b], Robert Hu[c]
[a]Institute of Astrophysics, National Taiwan University, Taipei, Taiwan.
[b]Chung-Shang Institute of Science and Technology, Longtan, Taiwan.
[c]Department of Electronics Engineering, National Chiao-Tung University, Hsinchu, Taiwan.

## ABSTRACT

NTU-Array is designed for W-band (78-113Ghz) interferometric observations of Sunyaev-Zeldovich effects. The first phase operation of the telescope with 6 receivers had its first light in 2008 with single-polarization and half the full bandwidth. The second-phase operation of NTU-Array in Nevada will begin the dual-polarization, full-band observation in 2010. One-bit sampling at 18Ghz and digital correlation are in use in this telescope. Due to the ultra broadband coverage, the IF system divides the 35GHz full-band into four 8.7GHz sub-bands. The first stage of IF module containing a 35GHz broadband amplifier with fairly flat-gain performance over 25db gain divides the first-stage IF into two outputs. The 2nd-stage IF module further divides the two input IF signals and down-converts them to four basebands of DC-8.7Ghz. An LO module with 8.7Ghz input is to generate outputs with x2, x3 and x9 harmonics for the down-conversion. The Walsh function is injected into the x9 LO via an IQ mixer. Each IF baseband is transmitted through an optical link to the 18Ghz, 1-bit sampling ADC located in the control room. The analog optical link contains a driver and equalizer to compensate for the path loss. Considering the limited size of the telescope mount, the entire IF/LO system of each receiver has a compact size about 20cm cubed. This physical size can be further reduced to fit the future 19-pixel-receiver upgrade of NTU-Array

## 1. INTRODUCTION

For efficient exploration of the anisotropy of cosmic microwave background radiation in the millimeter-wave frequency range, the receiver should be wideband as possible [1]. In the NTU-Array receiver, the incoming 78–113GHz millimeter-wave signal will first enter the cryogenic InP low noise amplifier (LNA) and then, through the transition of a stainless steel WR-10 waveguide, gets to the room-temperature W-band mixer [2]. The resulting DC–35GHz IF is then fed into the room-temperature wideband IF modules. Four separate base-bands are subsequently extracted by use of amplifiers, band-pass, low-pass filters, and three secondary mixers with the local oscillator (LO) frequencies at 17.4GHz, 17.4GHz and 26.1GHz, respectively.

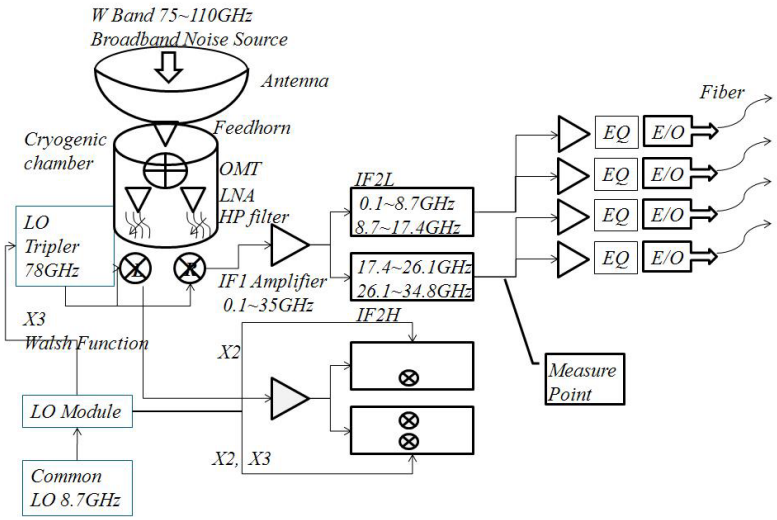


Figure 1. The NTU Array receiver schematics with RF (78.3GHz – 113.1GHz) to IF1 (0.1GHz-34.8GHz) to IF2 (0-8.7GHz) configurations

Millimeter, Submillimeter, and Far-Infrared Detectors and Instrumentation for Astronomy V,
edited by Wayne S. Holland, Jonas Zmuidzinas, Proc. of SPIE Vol. 7741, 774116

Each baseband bandwidth is chosen to be 8.7GHz to match the analog optical link bandwidth and the digital system sampling rate. The digital system includes ADC boards, FFT boards and correlator boards.

## 2. SYSTEM DIAGRAM

In the following section, detailed descriptions will be provided for the complete DC–34.8GHz sub-system, which also includes the LO and optical-link circuits. In addition, the measured results will be presented as well.

### 2.1 IF Modules

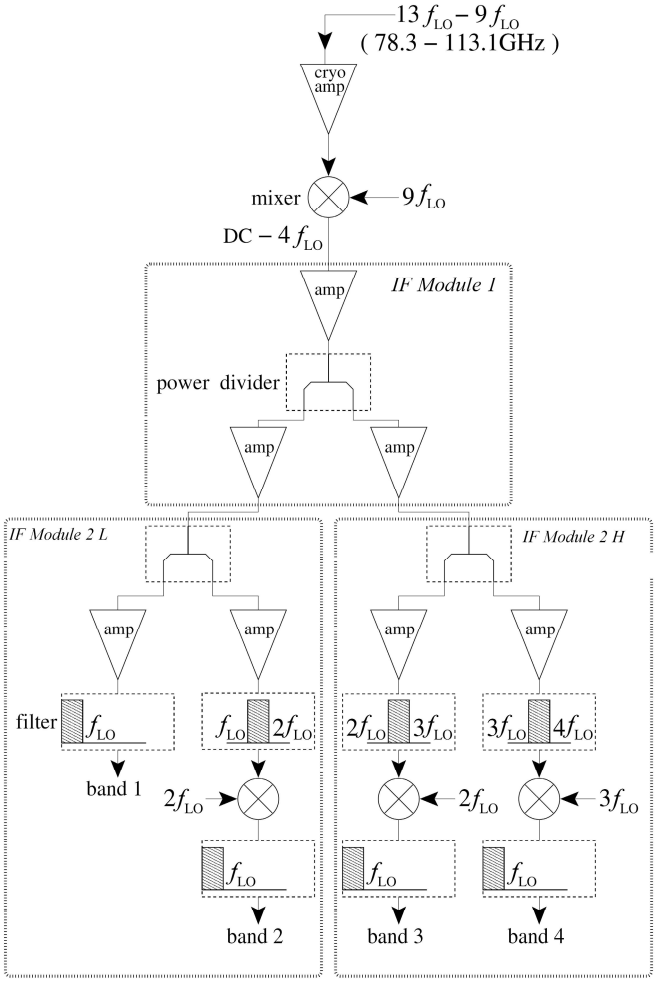


Figure 2. IF schematic diagram. The 0.1GHz to 35GHz IF signal was further down converted to four base bands with each base band covering 0 to 8.7GHz.

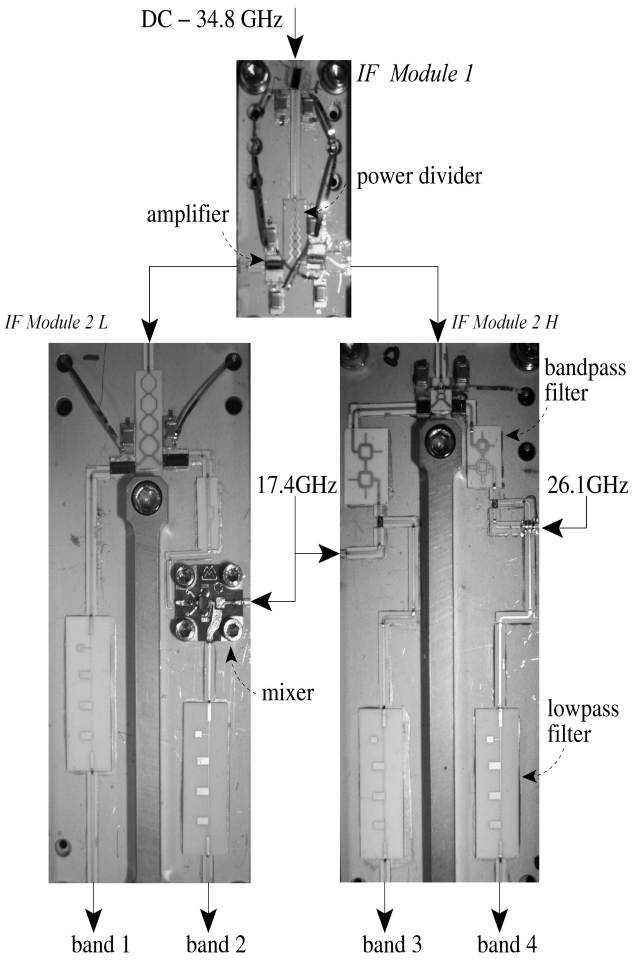


Figure 3. Photos of IF modules 1 and 2.

To retain the flexibility, core IF circuits are split into three modules. As shown in Fig. 2, the first module consists of a traveling-wave amplifier (Agilent AMMC5024), and then a multi-section 3dB wideband Wilkinson power divider with output ports connected to the same Agilent amplifiers. The substrate is made of 10-mil alumina ($Al_2O_3$) and the metal is gold. The output of 3dB power divider in IF module 2 L gets amplified by Hittite HMC462 on each of its branches. The DC–8.7GHz band 1 signal can now be extracted by using a low-pass filter; the 8.7–17.4GHz band 2 is obtained by using a band-pass filter, a mixer (Marki M1R0920) with 17.4Ghz $f_{LO}$ for down conversion, and finally a low-pass filter. The reason for not choosing 8.7GHz $f_{LO}$ to down-convert the second band is because such an LO frequency is bordering the

final DC–8.7GHz band, and any 8.7GHz LO leakage to the IF port will be difficult to remove; by contrast, the 17.4GHz LO is far away from the DC–8.7GHz band and can be easily suppressed later on should it leaks to the band.

The reason for there to be two identical amplifiers at the output of the power divider in IF module 2L, rather than the more straightforward arrangement of one amplifier followed by a power divider, is to eliminate the rippled response caused by the finite output-port isolation of the passive power divider itself. In the one-amplifier arrangement, for example, the reflected DC–8.7GHz signal by the band-pass filter on band 2 will be leaking into the other branch through the mixer and power divider and causes a rippled response on band 1. Likewise, the 8.7–17.4GHz signal reflected by the low-pass filter on band 1 can be coupled into band 2. In the two-amplifier case, the reflected signals from the two identical amplifiers will be indistinguishable. Since it is an even-mode excitation at the power divider's output ports, the cross coupling can be suppressed. With the same rationale, the IF module 2H has its power divider followed by two identical amplifiers (Eudyna FMM5709X). The mixers used in bands 3 and 4 are Hittite HMC292 and HMC329.

### 2.2 LO Module

Figs. 3 shows the schematic of the LO circuit where the 8.7GHz $f_{LO}$ is provided by a YIG oscillator. Note that the physical dimension of NTU-Array is relative small with the farthest receiver separation about 3 meter, the requirement for the phase noise level of LO is quite moderate, and a YIG with -110 dBc phase noise at 1Mhz is found adequate. The input power divider is followed by variable attenuators (TriQuint TGL4203) and amplifiers (Hittite HMC441). To have multiple medium power 17.4GHz outputs, the frequency doubler (TriQuint TGC1430F), medium power amplifier (TriQuint TGA9088A), a 17.4GHz narrow-band couple-lined filter, and Lange couplers (TriQuint TGB2001) are used here. On the second branch of the LO module, the 26.1GHz LO signal coming out of the frequency tripler (TriQuint TGC1430G) is sent into a medium-power amplifier (TriQuint TGA1073G) and then a 26.1GHz narrow-band coupled-line filter to remove possible harmonics. Multiple 26.1GHz LO signals are made possible by the use of Lange couplers (TriQuint TGB4001). The Walsh function modulated 26.1GHz (via Hittite HMC524 mixer) is then sent to an external tripler to generate the 78.3GHz LO for the front-end W-band mixer [3]. The LO signals provided by this module will be able to support two polarizations in each receiver.

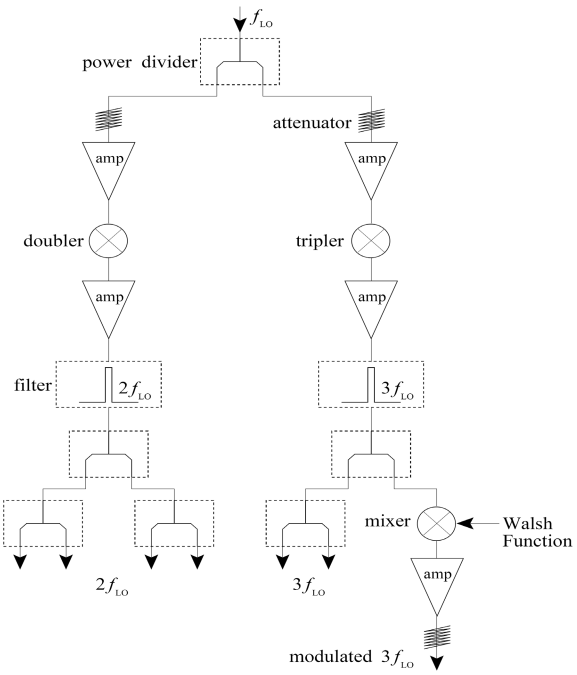


Figure 4. LO schematic diagram. All six receivers have a common 8.7 GHz LO source. The power of the input LO for each receiver is 8dBm.

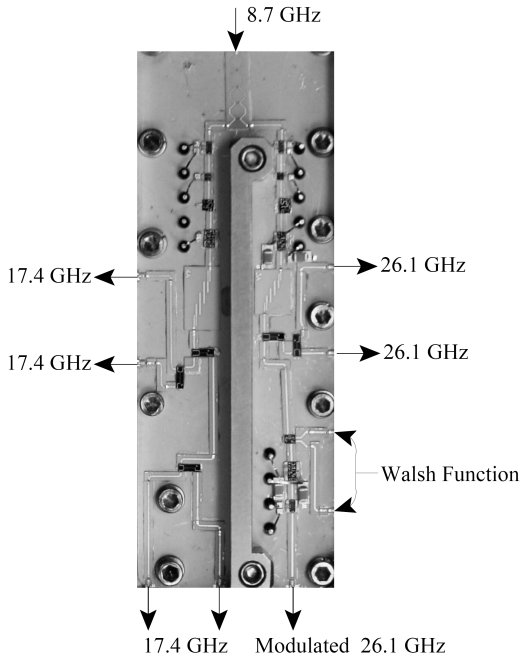


Figure 5. Photo of LO module. Each dual polarization receiver has one LO system supporting four 17.4 GHz LOs for Band 2 and 3, two 26.1GHz LOs for Band 4 and one 26.1GHz coded with Walsh function sent to the tripler to generate two 78Ghz LOs.

### 2.3 Optical link module

The four DC-8.7GHz base bands need to be transmitted to the control room for further digital processing. The only possible avenue is through an analog optical link of sufficient bandwidth. We chose the inexpensive Farbry-Perot optical transmitter (OEpic LF1130) and PIN optical receiver (OEpic LCF11) of digital communications at 1310nm for our analog link. The input P1dB power of the transmitter is determined to be 0dBm, which results in output power from the receiver around -14dBm, where the link noise is found around -35dBm across the 8.7GHz band. On the other hand, the ensuing ADC immediately after the optical link can correctly sample signals at a minimal power level of -20dBm. We thus fix the input of the optical link to -5dBm, so that the optical link stays in the linear regime with an output power sufficient to overcome the link noise. The 3dB bandwidth of the optical link is about 6.5Ghz, thus requiring a frequency equalizer to recover high frequencies.

The optical transmitter module consists of three stages of gain block amplifier (SNA176) and a passive equalizer to gets to the desired power level. Since the accumulation of the three cascading amplifiers reveals a discernible negative frequency slope, a gain equalizer is added, where the series *LC* is resonating at 8.7GHz and the quarter-wavelength transmission lines corresponds to that of 8.7GHz. At low frequency, this equalizer resembles a Π-shape resistive attenuator made of only $R_1$ and $R_2$; at 8.7GHz, the two ports of equalizer join together and low loss is expected [4].

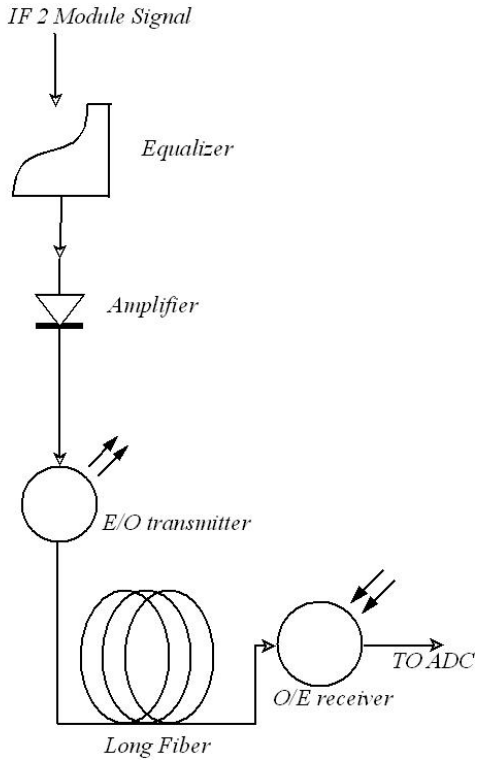


Figure 6. Optical link schematic diagram. The dynamical range of the optical transmitter is -5dBm to 0dBm. Equalizer and amplifier are used for supplying adequate power to supply the transmitter. The power optical receiver output minimum is -20Bm for the ensuing ADC to correct sample.

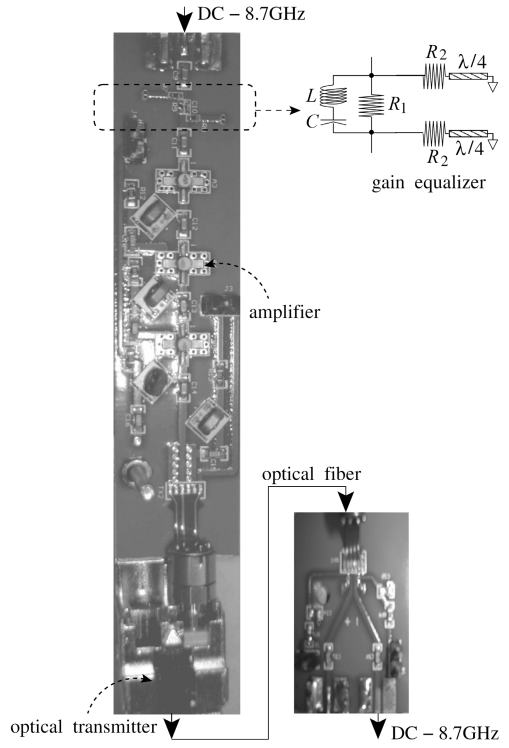


Figure 7. Photos of optical transmitter and receiver modules.

## 3. MEASUREMENT RESULTS OF THE IF/LO MODULE AND OPTICAL LINK PERFROMANCE

In this section, we show the lab measurement results of our IF/LO ystem. Figuire 8 indicates the IF/LO measurement setup and the measurement points.

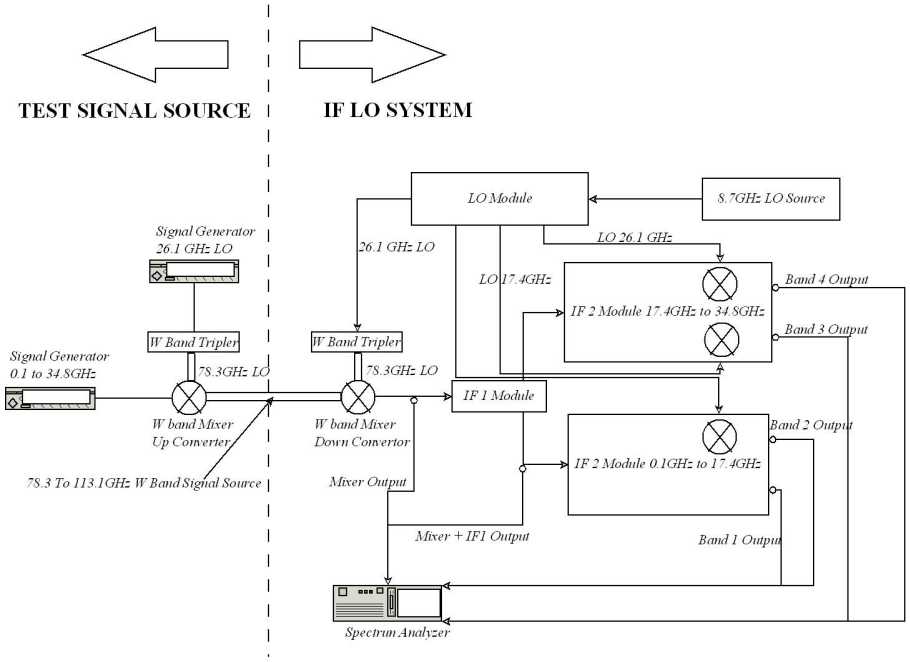


Figure 8. Measurement Setup diagram. The right is the full IF/LO system used in the NTU Array receiver. The left is the W-band signal source used for the tests, where the 0.1-34.8GHz CW signal is up-converted to 78.3 to 113.1GHz. The measurement points are marked with circles and connected to a spectrum analyzer.

### 3.1 Measurement results of the IF 1 Module

At the measurement points shown in Figure 8, the results are given in the Figure 9 to Figure14.

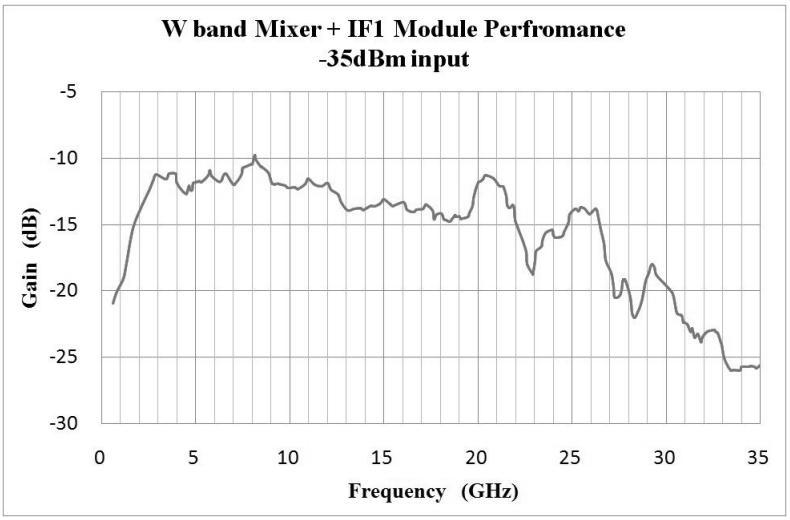


Figure 9. Measurement result of W-band mixer plus IF1 module. The spectrum shows about 5 dB slope from 2.5GHz to 19GHz. After 19GHz, it reveals resonances, creating 6dB variation in Band 3 (17.4 to 26,1GHz). The power rapidly declines in Band 4.

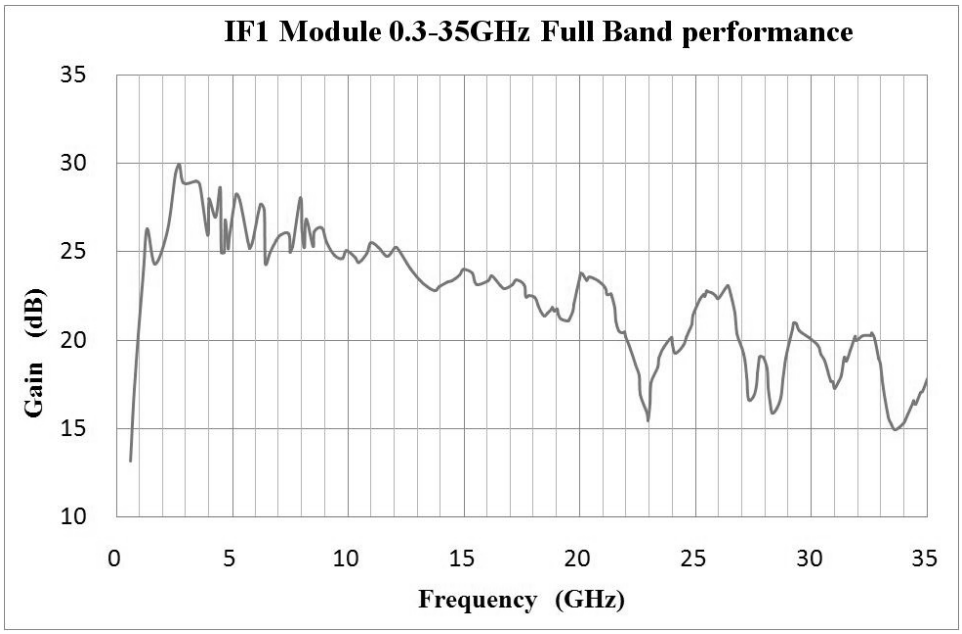


Figure 10. Measurement result of IF 1 module alone. The gain of IF 1 module is 25dB in Band 1, 23dB in Band 2, 20dB in Band 3 and 18dB in Band 4. The overall slope is 15dB from the band 1 to band 4 and resonances are seen in Bands 3 and 4.

### 3.2 Measurement results of the IF 2 Module

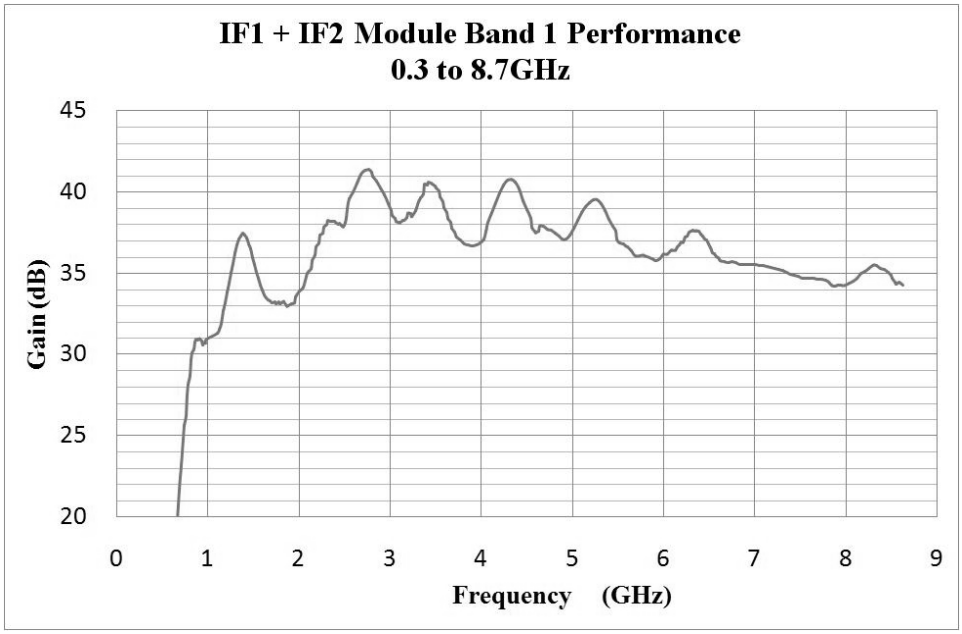


Figure 11. Measurement result for the IF 1+ IF2 module in Band 1, which shows a gain about 35dB and the slope is 5 dB.

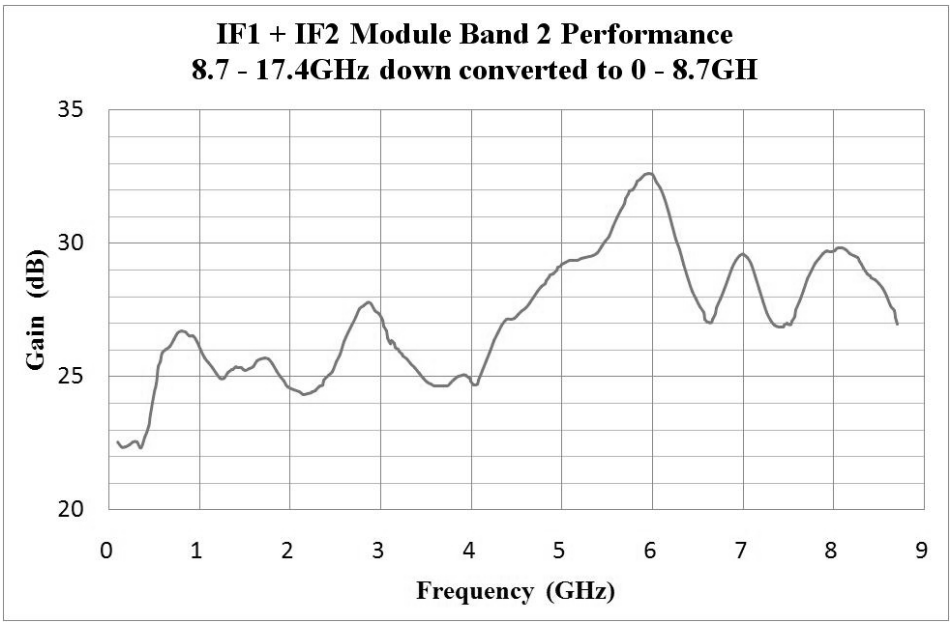


Figure 12. Measurement result of IF1 +IF 2 in Band 2, which shows a gain about 27dB. The spectral slope is inversed due to the 17.4 GHz LO at the upper spectral edge.

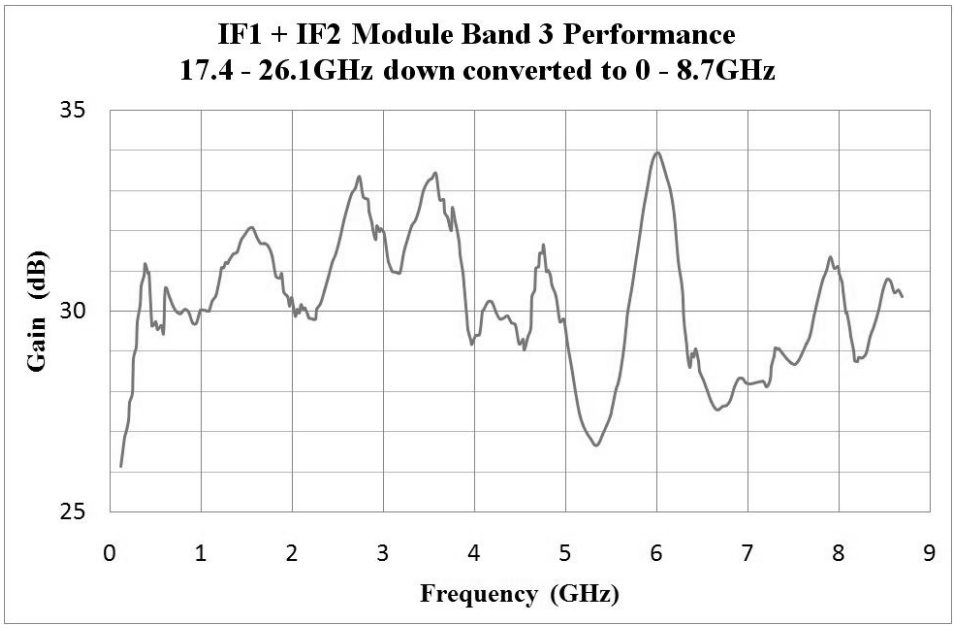


Figure 13. Measurement result of IF1 +IF2 in Band 3, which has a gain about 30dB and the slope about 1dB. The reflection in the module is obvious, corresponding to 5cm path length on the alumina substrate.

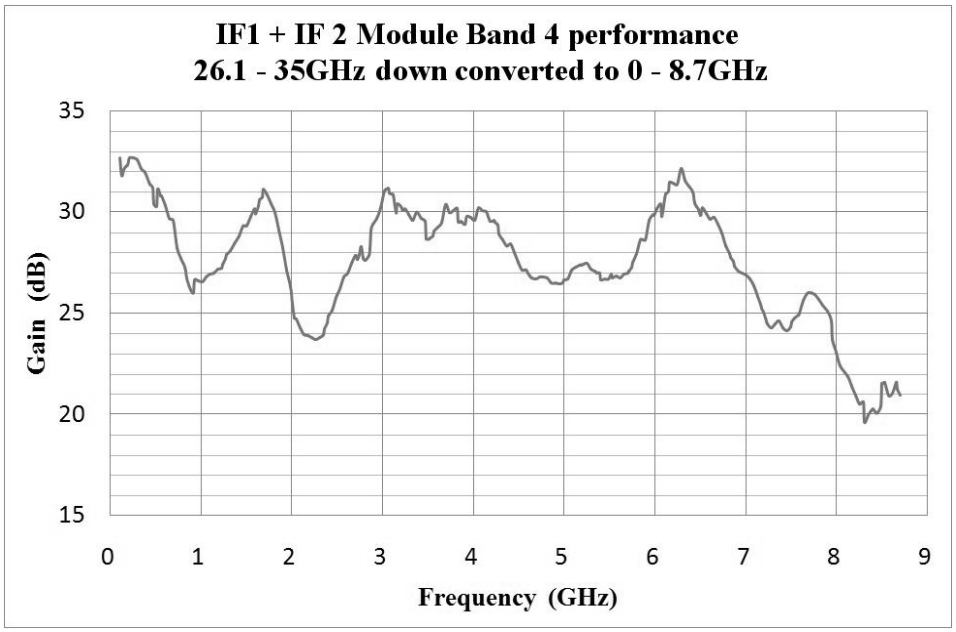


Figure 14. Measurement result of IF1 +IF2 modules in Band 4. The strong reflection occurring at 1GHz and 2.3GHz resemble that of Band 3. The power declines rapidly above 7Ghz.

### 3.3 Measurement result of the equalizer

The EQ and amplifier were used in cascade to compensate for the individual differences among different receivers and different IF bands. The equalizer aims to provide a 7dB slope as demonstrated in Fig.(15).

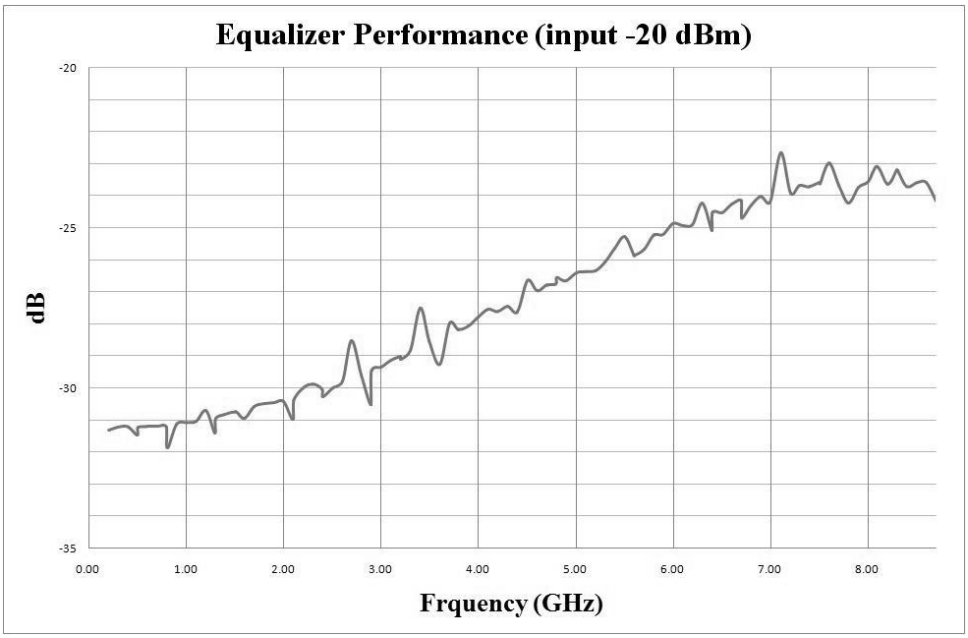


Figure 15. Performance of the equalizer. The equalizer has a 7dB slope from 0.3GHz to 8.7GHz. Depending on the output power from IF 2 modules, additional amplifiers with equalizers will be in use.

### 3.4 Measurement result of the optical system.

In view of the high loss of coaxial cables, the optical link system was chosen to carry the signal to the control room where back-end digital signal processors are located. The optical system is quite noisy with the total power about -35dBm dominated at frequency below 1GHz. Another critical consideration is that the optical transceiver was designed for digital communication and it limits our input power no more than 0dBm. The front end amplifier and equalizer were designed to match the optimum power. Figure 16 shows the result of optical system test.

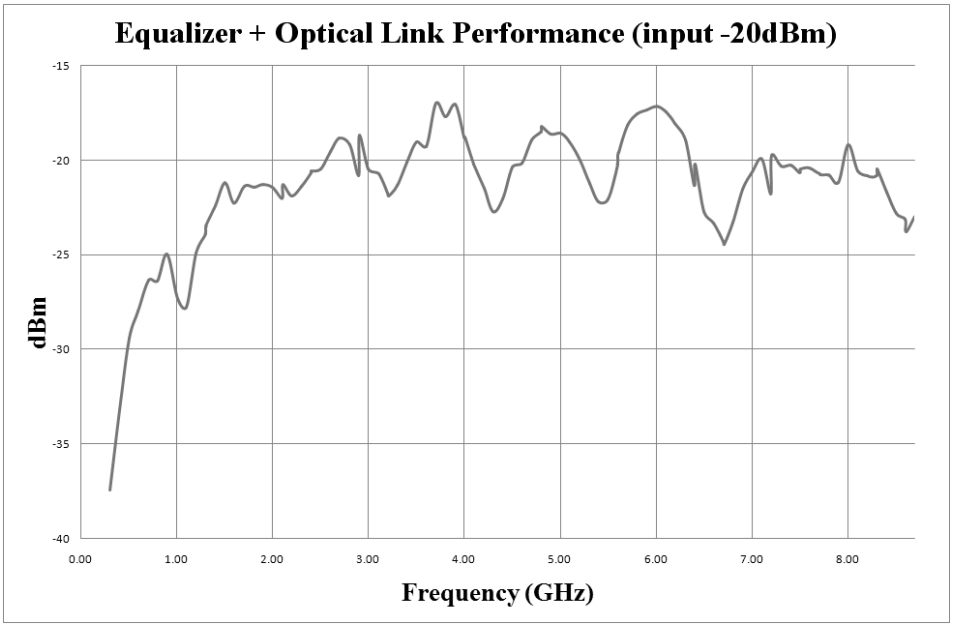


Figure 16. Measurement result for the optical system preceded by an EQ. The input power is -20dBm and the total gain is about -2dB. It shows that an EQ is necessary for optical link with a flat frequency spectrum.

## 4. MIRROR SIGNALS

Due to the imprecision in the cutoff of the frequency filters for band 2 to band 4, mirror signals in the adjacent bands can appear in-band. It is necessary to pin down the leakage of the mirror signals for calibration of the observation results. In addition, the mirror signal and the in-band signal are mixed at the same down-converted frequency; due to their being at the band edges of a filter, if the two mirror signals possess a finite relative phase, the complex correlation of the mixed signals will create unusual fringe patterns. Upon complex delay correlation, the in-band signals and mirror signals produce the real part of correlation,

$$A_R(\tau) = A(\cos(\omega\tau) + |\varphi_1||\varphi_2|\cos(\omega\tau + \delta)),$$

where A is the correlation amplitude of the in-band signals, $\varphi$: the fraction of mirror signal amplitude for receivers 1 and 2, $\omega$ the RF frequency, $\delta$ the phase difference of mirror signal between different receivers and $\tau$ is delay time for correlation. For the imaginary part,

$$A_I(\tau) = A(\sin(\omega\tau) - |\varphi_1||\varphi_2|\sin(\omega\tau + \delta))$$

Clearly, the real and imaginary parts of the delay fringes are not 90 degree out of phase as expected when $\delta$ is non-zero. Our tests include the measurement of phase difference $\delta$ and the fraction of the mirror signal to in-band signal $\varphi$.

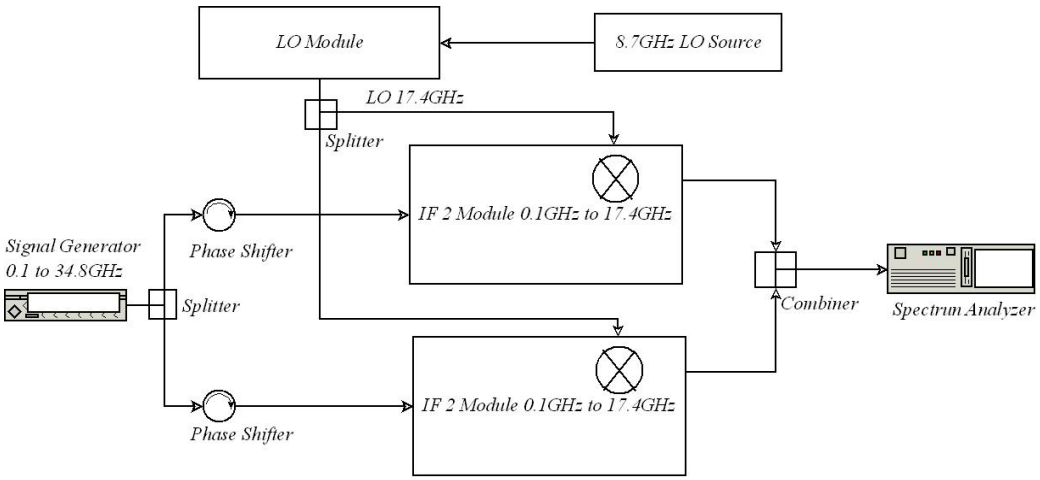


Figure 17. Measurement setup diagram. Signal generator is connected to the splitter followed by two phase shifters. The signals are sent to the IF2 modules for down conversion, and the converted signals are combined before sent to a spectrum analyzer to find out the combined power.

The setup for the measurement of δ is configured as Fig.(17). Upon combining the same signal through two different phase shifters and two different IF modules, the output power changes as the phase shifters change the relative path length. Our measured results are plotted in Fig.(18), where the output power is plotted against the phase shifter delay. We used the in-band signal to provide the correct delay phase, and then tested the mirror signals for possible additional 2 relative phase δ among different IF modules. One of the two measured IF 2 modules is fixed to be module 3, and all measurements for modules 1 and 2 are with module 3. The results reveal that δ is close to zero within ±10 degree, and according to the above equation, it will not produce additional phase in between the real and imaginary correlation, and the only effect is to enhance the amplitude of the real part of the correlation at the expense of reducing the amplitude of the imaginary part. Figure (19) reveals the degree and the range of mirror signal leakage. It will cause some loss of signal integrity in the range of leakage, but drift scan observations can help recover the signals to a certain degree.

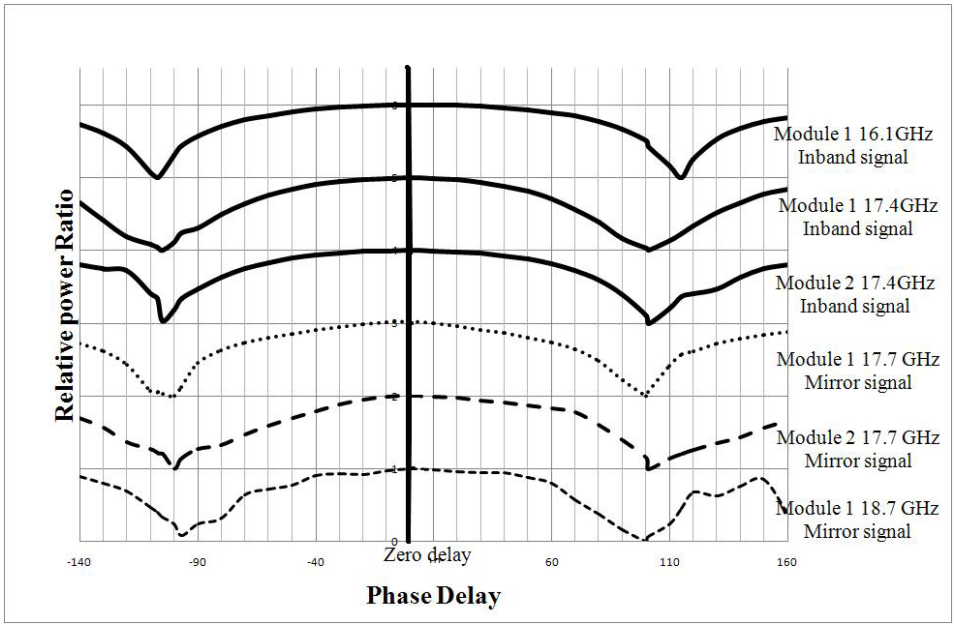


Figure 18. Measurement of the mirror signal phase difference δ for different IF2 modules, where modules 1 and 2 are separately measured against a reference module 3. The result shows that there is little phase difference, which also holds for the in-band signals in different modules.

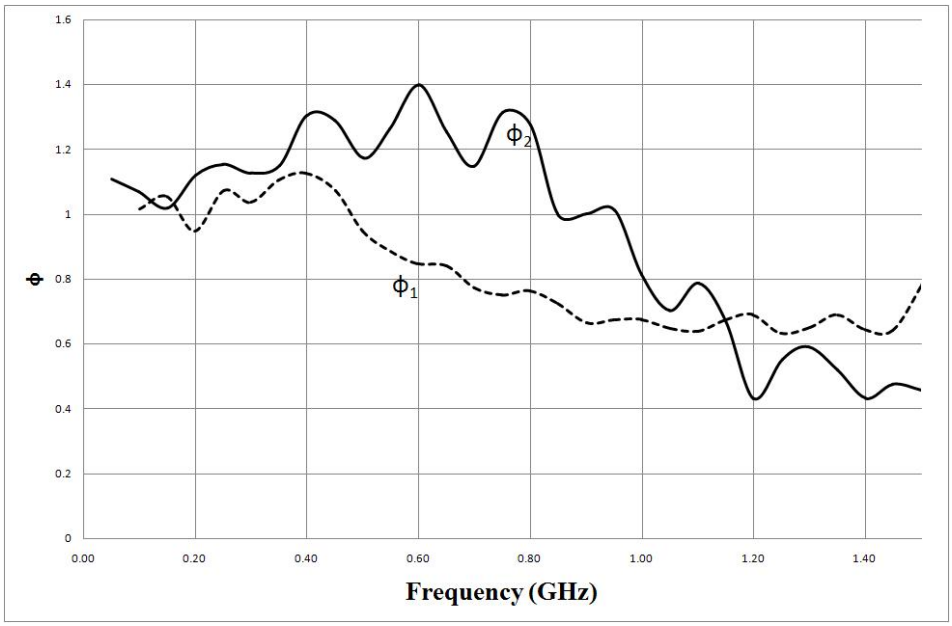


Figure 19: Measurement of the mirror signal amplitude fraction φ. Unlike the phase measurement given in Fig.(18), the result is quite variable for different receiver; some show that the mirror signal is stronger than the in-band signal below 800MHz. After1.1GHz, the fraction is down to at least 0.7.

## 5. CONCLUSION

The performance of the full-band IF/LO system have been fully tested. The test results for the ensuing back end digital system was also completed and reported in this conference [5]. Despite the full band IF exhibits rather non-uniform spectrum, those of individual base bands are not as bad. It has been evaluated that a one-bit correlator can tolerate input spectral non-uniformity to a fairly high degree. For example, a 10 dB slope will only degrade the signal-to-noise ratio by a factor of 20% or so [6]. On the other hand, the mirror signal leakage can severe impair the conventional interferometry observation, where the sky is kept stationary relative to the telescope. This is because a stationary measurement requires both real and imaginary parts of correlation to be detected in order for it to disentangle the phase and amplitude of a Fourier component. With the mirror leakage where the imaginary part is degraded, it becomes difficult to determine the Fourier component from interferometry observation. However, drift scan observations can help alleviate this problem. When the sky becomes time-dependent, it is possible to determine the phase and amplitude separately from the fringes, even with only the real part of the correlation. This drift scan method works better for long baselines than for short baselines.

The physical dimension of the present IF/LO module is relatively compact, about 20 cm cubed in volume. As the trend of the future CMBR observation with coherent detectors shifts toward multiple-pixel receivers, the IF/LO module will need to be further reduced in size. We are funded in 2009 to build a prototype array with dual-polarization multi-pixel receivers, where the pixel number is 19. Unlike the present IF/LO module where most chips are from commercial sources, redesigns of RF, IF and LO chips are underway, with an aim to make it as much system-on-chip as possible. We target at an IF/LO module for the entire 19 pixels no more larger than the present IF/LO module.

## REFERENCES

[1] A. R. Thompson, J. M. Moran, G. W. Swenson, Interferometry and Synthesis in Radio Astronomy, 2nd edn. (Wiley, 2001).

[2] N. R. Erickson, R. M. Grosslein, R. B. Erickson, S. Weinreb, A cryogenic focal plane array for 85.115GHz using MMIC preamplifiers, IEEE Trans. Microwave Theory Techniques, vol. 47, no. 12, pp. 2212–2219. (Dec. 1999)

[3] J. Granlund, A. R. Thompson, B. G. Clark, "An application of Walsh functions in radio astronomy instrumentation," *IEEE Trans. Electromagnetic compatibility,* vol. EMC-20, no. 3, pp. 451–453. (Aug. 1978)
[4] D. J. Mellor, "On the design of matched equalizers of prescribed gain versus frequency profiles," *MTT-S Digest,* vol. 77, pp. 308–311. (June 1977)
[5] S. K. Wong, et al., "Real-Time Tbps Digital Correlator in NTU-Array ", SPIE conference, this volume (2010)
[6] S. K.Wong and T. Chiueh, ""Effects of Non-uniform Input Spectra on Signal-to-Noise Ratio in Wide-Bandwidth Digital Correlation", PASP, vol. 122, pp. 215-223 (2010)